Covalent Incorporation of Trehalose within Hydrogels for Enhanced Long-Term Functional Stability and Controlled Release of Biomacromolecules

HHS Public Access

Author manuscript

Adv Healthc Mater. Author manuscript; available in PMC 2016 April 08.

Published in final edited form as:

Adv Healthc Mater. 2015 August 26; 4(12): 1802–1812. doi:10.1002/adhm.201500334.

Covalent Incorporation of Trehalose within Hydrogels for Enhanced Long-Term Functional Stability and Controlled Release of Biomacromolecules

Timothy M. O'Shea,

Harvard–Massachusetts Institute of Technology Division of Health Sciences and Technology, Institute for Medical Engineering and Science, Massachusetts Institute of Technology, Cambridge, MA 02139, USA

David H. Koch Institute for Integrative Cancer Research, Massachusetts Institute of Technology, Cambridge, MA 02139, USA

Matthew J. Webber,

David H. Koch Institute for Integrative Cancer Research, Massachusetts Institute of Technology, Cambridge, MA 02139, USA

Department of Anesthesiology, Children's Hospital Boston, 300 Longwood Avenue, Boston, MA 02115, USA

Alex A. Aimetti, and

InVivo Therapeutics Corporation, One Kendall Square Building 1400 East, Floor 4, Cambridge, MA 02139, USA

Robert Langer

Harvard–Massachusetts Institute of Technology Division of Health Sciences and Technology, Institute for Medical Engineering and Science, Massachusetts Institute of Technology, Cambridge, MA 02139, USA

David H. Koch Institute for Integrative Cancer Research, Massachusetts Institute of Technology, Cambridge, MA 02139, USA

Department of Chemical Engineering, Massachusetts Institute of Technology, Cambridge, MA 02139, USA

Robert Langer: rlanger@mit.edu

With the advent of the biotechnology industry, numerous biopharmaceutical products in the form of peptides, proteins, antibodies, enzymes, engineered fusion proteins, and conjugates have been developed for the treatment of diabetes, inflammatory and metabolic diseases, as well as various cancers and neurological disorders.[1–5] The advantages of protein therapeutics compared to traditional small molecule drugs include higher potency, a reduction in toxicity and off target effects, and a more predictable mechanism of action.[5,6]

Correspondence to: Robert Langer, rlanger@mit.edu.

Supporting Information

Supporting Information is available from the Wiley Online Library or from the author.

These favorable properties have allowed protein therapeutics to achieve higher clinical trial success rates and faster regulatory approval timelines compared to all other classes of drugs in recent times.[4,7] However, in spite of the encouraging clinical results, there still remain several manufacturing, storage, formulation, and administration challenges that hamper their effectiveness across a wider spectrum of indications. Owing to limitations in oral and parenteral administration, biomaterial-based drug delivery systems (DDS) such as liposomal and polymeric nanoparticles, hydrophobic polymer matrices, as well as locally applied injectable hydrogels have been developed to avoid undesirable repeat injections of drug-only solutions.[8–11]

Hydrogel materials have received the most attention within the context of controlled release of biologic therapeutics, and numerous systems have been developed affording significant temporal control and localized bioavailability of these drugs.[11,12] Nonetheless, for a number of particularly fragile biomacromolecules, whose activity depends on precise structural folding and/or the specific arrangement of cofactor molecules, current hydrogel technology is inadequate. These complex biomacromolecules, which include monoclonal antibodies and therapeutic enzymes, have seen limited successful incorporation within hydrogels as they readily lose functional activity during biomaterial encapsulation and/or the controlled release period.[13–15] Additionally, irreversible denaturation or aggregation of these proteins may also pose significant toxicity and undesirable immunogenic risks.[6] Understanding how existing hydrogel technologies disrupt protein integrity is essential for the development of viable solutions. Hydrogels formed using covalent crosslinking chemistries have the potential to react and alter proteins. Specifically, proteins can be irreversibly modified by: i) free radical attack in photoinitiated hydrogels;[16,17] ii) the formation of undesirable protein–polymer conjugates in systems which employ certain amine or thiol-reactive chemistries;[18–20] as well as iii) disulfide interchange in free thiol containing systems. In physical gels that are formed using amphiphilic molecules, strong hydrophobic interactions needed to facilitate network formation can disrupt protein structure.[21] Moreover, there is currently limited understanding pertaining to long-term protein stability within hydrogel matrices where a multitude of potential biomaterial—and in vivo—derived forces such as material-drug electrostatic or hydrophobic interactions, thermal-induced protein misfolding, hydrolytic degradation, deamidation, and disulfide interchange can contribute to loss of protein activity.[10,22]

To protect proteins from these structural perturbing sources, small molecule osmolytes such as sugars, polyols, and salts have been employed as stabilizing agents.[23–25] However, incorporating such a stabilizing mechanism within prolonged release hydrogels with high water content presents challenges. Specifically, small molecule excipients diffuse from hydrogel systems more quickly than the larger biomacromolecules requiring stabilization. Protein stabilization is therefore difficult to maintain beyond the initial formulation and delivery period. As a result of the inadequacy of small molecule excipients for enduring stabilization within biomaterial matrices, the development of strategies to preserve long-term protein bioactivity is an important area of investigation.[22,26]

Here, we describe a new method for the long-term stabilization of protein therapeutics within hydrogel networks through the covalent incorporation of trehalose, a well-

characterized nonreducing disaccharide known to be an extremely effective protein-stabilizing excipient,[27,28] into a synthetic polymeric hydrogel. Using diacrylate functionalized trehalose monomers we covalently incorporated the excipient into the network of a known biocompatible thiol-ene ethoxylated polyol (EP) hydrogel platform to form a biodegradable, nonswelling material.[12] The trehalose hydrogel affords prolonged stabilization of model protein therapeutics throughout a period of controlled release, as well as under relevant formulation and shelf-life stressors that include heat and lyophilization. The strategy described here for trehalose incorporation within a hydrogel illustrates a robust method that could be applied to a variety of formulation, manufacturing, and delivery applications of protein therapeutics.

To synthesize diacrylate functionalized trehalose (TDA) for covalent incorporation within the ethoxylated polyol hydrogel, we adapted a synthetic scheme described previously by Dordick and colleagues involving the acylation of trehalose by vinyl acrylate (Figure 1a).[29] By using Candida Antarctica Lipase B (CALB) immobilized on acrylic resin, we achieved regiospecific esterification of the trehalose at only the 6 and 6′ hydroxyl sites to synthesize a diacrylate functionalized trehalose without requiring protection/deprotection steps often required in the chemical modification of carbohydrates[30] (Figures S1 and S2, Supporting Information). Next, we fabricated the trehalose hydrogels by combining the TDA monomer with specific tri-thiol-functionalized ethoxylated polyol esters oligomers (TEPEs) derived from a library used to form hydrogels via a thiol-ene Michael addition reaction.[12] Specifically, for the trehalose hydrogel system reported here, we applied trimethylolpropane ethoxylate thiolactate (TMPE-TL) as the thiol-functionalized crosslinker as well as poly(ethylene glycol) diacrylate (PEGDA575) to create materials with varied ratios of PEG to trehalose within the network (Figure 1a). Herein, we denote hydrogel formulations in terms of the percentage of diacrylated molecules attributed to the TDA (i.e. 100% trehalose hydrogel (100T) has 100% acrylate groups from TDA). Combining TMPE-TL with mixtures of PEGDA and TDA at thiol and acrylate functional group stoichiometric equivalency under physiologically buffered conditions (1× Phosphate buffered saline, pH = 7.4 (PBS)) resulted in an increasingly viscous solution which cured in situ to form a hydrogel within 2–3 min of mixing. Dynamic rheology was used to monitor the kinetics of gelation for the trehalose hydrogels. 100T hydrogels displayed a sol–gel transition and *as cured* network mechanical properties comparable to previously reported ethoxylated polyol (EP) hydrogels (Figure 1b).[12] In addition, the kinetics of gelation showed minimal deviation across the various TDA/PEGDA ratios investigated, suggesting that the electrophilic characters of the TDA acrylate groups were comparable to those on the PEGDA (Figure S3, Supporting Information). The equilibrated swelling ratio, Q_m, for the trehalose hydrogels increased with higher TDA content (Figure S4, Supporting Information). Furthermore, trehalose hydrogels (25 wt%) formulated at less than or equal to 75T showed syneretic behavior at 37 °C (Figure 1c). Much like the EP hydrogels reported previously, trehalose hydrogels that demonstrated initial syneresis upon equilibration also displayed nonswelling degradation via an ester hydrolysis mechanism[12] (Figure S5, Supporting Information). The rate of degradation of trehalose hydrogels was proportional to the percentage content of TDA. The faster degradation observed in hydrogels with increasing ratios of TDA was attributed to the more labile ester bonds from the TDA as well as the increased Q_m values, which corresponds to

higher free water content in the equilibrated network (Figure S6, Supporting Information). Throughout the complete hydrogel degradation process, trehalose persisted, and was detectable, within the network (Figure S7, Supporting Information).

To characterize the influence of TDA content on model protein release from hydrogels, we next encapsulated FITC labeled ovalbumin ($M_W \approx 45$ kDa) and Alexa Fluor 647 conjugated IgG ($M_W \approx 150$ kDa) within various trehalose hydrogel formulations and quantified release in vitro via fluorescent intensity measurements. The hydrogels displayed triphasic release profiles that were fitted to a Weibull distribution[12] (Figure 2a). For ovalbumin-loaded hydrogels increasing the TDA content led to exponentially decreasing t_{50} (time to 50% release of drug) values, while k (the molecule release constant) increased linearly (Figure S8, Supporting Information). The release kinetics were comparable for proteins of dissimilar size (ovalbumin and IgG), indicating the controlled release from the network was primarily dependent on network degradation rather than the passive diffusivity of the protein (Figure 2b). The accelerated release kinetics observed for hydrogels with increasing TDA content was reminiscent of that seen when we previously blended ratios of TMPE-TL with the faster degrading TEPE, trimethylolpropane ethoxylate thioglycolate (TMPE-TG).[12] From this observation, we established formulation parameters allowing us to match the release kinetics for several trehalose hydrogels with a corresponding TMPE-TG/TL blend-PEGDA 575 material (Figure 2c). Specifically, 50T trehalose hydrogels had protein release and degradation profiles similar to that of a 30/70 TMPE-TG/TL 575 blend while the 25T formulation was equivalent to the 15/85 mixed hydrogel. By matching hydrogel degradation and protein release kinetics in hydrogels with and without trehalose, we could now probe whether covalent trehalose incorporation would be beneficial to long-term protein stability with minimal potentially confounding variables.

With matched release kinetics for trehalose and EP hydrogels obtained, we next turned our attention to the effect of trehalose network incorporation on the functional activity of delivered proteins. To perform the protein activity preservation/recovery assays, we used a commercially available horseradish peroxidase (HRP) isoform C as the first model protein. This 40 kDa protein is similar in size to the FITC-labeled ovalbumin used to characterize the controlled release kinetics and possesses complex structural features that make it a good model protein for analyzing the influence of various hydrogel properties on protein stability. Specifically, the protein is a metalloenzyme with an active site, a noncovalently bound heme prosthetic group, which allows the protein to catalyze the removal/conversion of hydrogen peroxide to oxidize numerous organic and inorganic molecules. The protein also contains four disulfide bonds and numerous metal-binding sites that attract two divalent calcium ions to bind to the protein as enzymatic cofactors. Conformational or structural perturbations of these important elements result in loss of protein activity. For example, depletion of bound calcium ions due to structural instabilities can reduce the activity of the protein by over 50% while heme group displacement or destruction can also substantially affect protein function.[31–33] Therefore, given the many ubiquitous features of this protein (metal/heme cofactors, the presence of numerous disulfide bonds, dominant alpha helix secondary structure) HRP represents a good first protein to evaluate the efficacy of trehalose hydrogels. Furthermore, others have documented the enhanced stabilizing effect of trehalose and trehalose polymers on HRP activity in aqueous solution upon application of heat and

lyophilization stressors which enables benchmarking of the current hydrogel technology.[34–37] Prior to hydrogel encapsulation, we first characterized the solution stability of HRP at 37 °C as well as against dialysis (10 kDa cut-off) to drive the displacement of bound cofactors (Figure S9, Supporting Information). The thermal stability of HRP in solution was significantly concentration dependent. Specifically, 1 mg mL^{-1} solution of HRP showed no significant loss of activity over an incubation period of 1 week, while activity decreased significantly in solutions of 100 μg mL^{-1} (45% activity loss over first 24 h) and 10 μg mL^{-1} (80% activity loss after just 24 h). Furthermore, dialysis of 100 μg mL^{-1} solution accelerated this loss of activity over the subsequent days of incubation (Figure S9, Supporting Information). These findings demonstrate that HRP is a highly unstable protein at physiological temperatures in dilute solutions and support its use for the long-term release stability studies.

Next, we evaluated the recoverability of active HRP released from trehalose and EP hydrogels in vitro. Using 60 μL hydrogel discs, we encapsulated 2 mg mL^{-1} of HRP and incubated samples in 600 μL PBS/0.01% BSA at 37 °C to simulate physiological conditions. HRP activity was assessed upon daily replacement of incubation media using a standard HRP substrate solution, 3,3′,5,5′-tetramethylbenzidine (TMB). The percent recovery of active HRP was directly related to the trehalose content within the hydrogels (Figure 3a). When loaded with 2 mg mL^{-1} HRP, the 100T hydrogels allowed for practically total recovery of HRP over a 5 d period. By comparison, 50T hydrogels showed approximately 50% recovery of HRP when loaded at the same concentration, with detection of additional active HRP limited after approximately 10 d with this material. The recovery was reduced dramatically with 25T hydrogels allowing only 7% of total active HRP to be recovered. Although suggestive of improved HRP stability, we are mindful that these studies are influenced by the degradation rate of the material which is affected substantially by total trehalose content. To control for the kinetics of network degradation, we compared a 50T hydrogel with the corresponding blended EP hydrogel. Within this comparative study the 50T hydrogel demonstrated significantly superior recovery of active HRP compared to the EP hydrogel independent of HRP loading (Figures 3b and S10, Supporting Information). Specifically, at 2 mg mL^{-1} loading concentration recovery of active HRP was nearly sevenfold more for the 50T hydrogels (47.5%) compared to the EP material (7% HRP activity recovered). For all hydrogels the cumulative recovery showed a triphasic profile with similar kinetic parameters to the FITC-ovalbumin release assays. However, active HRP recovery profiles demonstrated lower t_{50} values and a faster rate of third phase decay compared to the FITC-ovalbumin release curves. The differences in the active HRP release kinetics compared to that of total protein release suggest that more significant HRP destabilization is occurring within both hydrogel groups at later incubation time points during the terminal hydrogel degradation phase. This enhanced protein destabilization is likely caused by the increased concentration of carboxylate functional groups within the network which are created as a result of network hydrolysis. The specific chemical mechanism by which these carboxylate groups may disrupt the integrity of HRP pertains to the chelation of bound calcium cofactors and is explored in more detail within the subsequent paragraph. Protein loading also influenced recovery of active HRP, with a higher trehalose to protein ratio resulting in increased recovery (Figure 3c). Explicitly, a fourfold

reduction in protein concentration (from 2 mg mL^{-1} to 500 μg mL^{-1}) resulted in a nearly 15% increase in normalized protein activity but with equivalent release kinetics. To assess the effect of possible disulfide interchange between the protein and residual thiol groups within the hydrogel, we formed 50T hydrogels with varying degrees of TMPE-TL excess. The presence of free thiol groups within the hydrogel network was confirmed by Ellman's assay and can be visualized as a yellow staining of the material (Figure 3d). Unsurprisingly, increased free pendant thiols within the network significantly diminished total HRP recovery (Figure 3d). This result is consistent with other reports that have observed a loss of HRP activity in the presence of thiol reducing agents such as dithiothreitol (DTT).[38] Taken together these results demonstrate that covalently incorporating trehalose into the hydrogel leads to improved recovery of active HRP in a manner that is dependent on trehalose concentration, network chemical composition, and protein-loading parameters.

To elucidate the mechanism by which covalent trehalose incorporation within hydrogels improves the functional HRP recovery during controlled release, we attempted to characterize protein secondary and tertiary structure within the hydrogel. Circular dichroism (CD) demonstrated preservation of protein structural signals during gelation but upon hydrogel equilibration scattering from the material limited further analysis (Figure S11, Supporting Information). FTIR analysis was used to evaluate protein secondary structure on dehydrated hydrogel samples, but low sensitivity and interference from hydrogen bonding of the trehalose within the network made the analysis inconclusive. Evaluation of the absorbance of the Soret band occurring around 400 nm wavelength provided some insight into the stability of the heme ring within HRP. Minimal attenuation or shifting of this visible signal attributed to the prophoryin ring was detected in either the trehalose or EP hydrogel samples over time suggesting minimal disruption of this structure (Figure S12, Supporting Information). To investigate whether the hydrogel caused depletion or displacement of calcium cofactors bound to HRP, a comparative study was performed whereby hydrogels were incubated in media containing calcium ions and total active HRP recovery was quantified. Interestingly, the recovery of HRP was significantly higher for EP hydrogels incubated within the calcium-containing media. Specifically, over the first 4 d of incubation the EP hydrogels showed equivalent HRP recovery to that of the trehalose hydrogel and prolonged recovery of active HRP within these hydrogels was observed up until terminal degradation at 2 weeks of total incubation (Figure 3b). As a result, approximately 48% of total active HRP was recovered from the EP hydrogels incubated in the calcium containing media. Despite this increased recovery, following the first 4 d of incubation the inclusion of calcium in the media was unable to provide the stabilization required to achieve the same levels of recovery as seen in the trehalose hydrogels (Figure 3b). Within the calcium-containing media trehalose hydrogels demonstrated close to total recovery (97.5%) of active HRP over a 2 week period. The additional stabilization in the calcium media for the 50T hydrogels was detectable only after 6 d of incubation. After 6 d the active HRP recovery in PBS began to decay rapidly while in the calcium media the active recovery curve followed the same trend as total protein release. Taken together, these results suggest that at early stages of incubation there are potentially reversible structural perturbations of HRP within the EP hydrogel that displaces calcium ions from the metal binding site of the protein, which is recoverable provided renewed sources of these ions are accessible to the protein. However,

other structural perturbations that are either nonreversible or that are calcium ion binding site independent must also take place within the EP hydrogel to account for the near 50% unrecovered HRP noted when incubated in calcium media. The variation in total recovery for trehalose hydrogels within the two medias suggests that, at least initially, the trehalose provides a stabilizing effect on HRP that is media independent. However, as the material starts to degrade the presence of excess calcium ions acts to mitigate some protein destabilization occurring within the hydrogel. It is hypothesized that an excess presence of divalent cations in the media acts to overcome chelation of HRP-bound calcium that may be readily caused otherwise by the increased concentration of carboxylate anion hydrolysis products locally within the hydrogel. This chelation theory is further supported by an observed slowing of the hydrogel degradation rate for both hydrogel groups in calcium-containing media suggesting the possible formation of stabilizing ionic salt bridges involving the divalent cations and the carboxylate hydrolysis products. While beyond the scope of this paper, applying new emerging protein spectroscopy techniques could be used in the future to better understand the specific structural stabilization afforded by the trehalose hydrogels in situ.[39,40]

Given that as an osmolyte trehalose has demonstrated effective stabilization across a variety of different classes of proteins and enzymes, we hypothesized that covalent incorporation of trehalose into hydrogels would be equivalently robust. To determine whether this was an accurate assessment, we next quantified active protein recovery during controlled release for several other well-characterized model enzymes. For glucose oxidase (GOx), a 130 kDa dimeric enzyme with a Flavin adenine dinucleotide (FAD) redox cofactor, the trehalose hydrogel resulted in enhanced recovery compared to the EP hydrogel over a 2 week period (Figure 3e). Using an Amplex red assay to quantify active GOx, trehalose hydrogels showed 65% total cumulative recovery that was more than double that seen for the EP hydrogel (26%). The kinetics of release for this large protein were also triphasic, but compared to HRP all active release of GOx occurred as a result of network degradation rather than diffusion. For α-chymotrypsin, a serine protease with dominant Beta sheet structure, the enzyme itself caused faster network hydrolysis and consequently more rapid protein release (Figure S13, Supporting Information). However, even with a rapid first-order release profile a higher recovery of active protein in the trehalose hydrogel was observed. These additional protein studies demonstrate a robust stabilizing effect attributable to the covalent incorporation of trehalose into the hydrogel network.

Despite the positive release assay results these studies could not confirm whether stabilization of protein is conferred by the trehalose hydrogel itself or by trehalose-containing network degradation products that diffuse into the incubation media along with the protein. To quantify stabilization of HRP within trehalose hydrogels, we prepared 15 μL hydrogel discs and conducted in vitro activity examinations whereby we sacrificed triplicate hydrogels every 2 d and incubated the material in TMB substrate solution to evaluate total activity. When placed in the TMB solution, hydrogels with active HRP turn a deep blue and the converted chromophore diffuses into the incubation solution increasing the readable signal of the solution. After 5 min the substrate solution was quenched with acid and the gel removed from the media before the solution was read on a microplate reader. Due to high HRP loading within hydrogel samples (1 mg mL^{-1}), both trehalose and EP hydrogels were

at the detection limit of the assay at the time of curing. HRP activity in the 50T hydrogels remained at the detection limit for up to 6 d of incubation in vitro before beginning to decrease, likely resulting from protein release into the incubation media as the material begins to degrade around this time (Figure 4a). By contrast EP hydrogels with and without soluble trehalose showed significantly decreased activity from encapsulated HRP after just 48 h with activity continuing to decay exponentially over the subsequent 12 d period (Figure 4a). The incorporation of soluble trehalose within EP hydrogels did not enhance protein activity likely due to its rapid diffusion from the network during the initial incubation. These data complement the HRP release assay results and together demonstrate preservation of HRP activity in vitro that can only be attributed to the covalent incorporation of trehalose within the hydrogel network.

To evaluate whether covalent trehalose incorporation had similar stabilizing effects in vivo, we implanted hydrogels containing HRP subcutaneously in mice. The 15 μL hydrogel discs loaded at 2 mg mL^{-1} were retrieved at 2, 4, 8, and 10 d postimplantation and evaluated for HRP activity using the same TMB assay. In contrast to in vitro experimental results HRP activity was maintained at much higher levels for longer periods of time within both hydrogel groups in vivo. At 2 and 4 d, the HRP activity within both trehalose and EP hydrogel samples was equivalent. However, by 8 and 10 d following implantation, significantly higher activity was observed in the 50T hydrogels (Figure 4b). Whether this differential activity is attributed entirely to an enhanced stabilizing effect of the trehalose is uncertain as the 50T hydrogels appeared to degrade slower than the EP hydrogels, in spite of this parameter having been matched in vitro. This finding could suggest that the trehalose hydrogel was less susceptible to sources of in vivo hydrolysis, such as endogenous esterases, than the EP hydrogel and warrants further investigation. The increased duration of HRP preservation in vivo in both hydrogel groups is likely a function of slower material degradation and reduced HRP release from the hydrogel. Slower release kinetics could be attributed to less sink-like conditions within the mouse subcutaneous space. Additionally, HRP activity preservation may be augmented by endogenous divalent cations such as Mg^{2+} and Ca^{2+} which may offset the chelating effect of the hydrogel degradation products on HRP bound calcium cofactors. Overall, these in vivo studies confirm predictions based on results in vitro as protein activity was preserved in both environments as a result of covalent incorporation of trehalose within the hydrogel network.

In considering the translational potential of the trehalose hydrogel platform, we wanted to evaluate the stabilization of proteins upon application of various possible stressors that proteins may experience during biotherapeutic formulation, shelf-life, and transportation processes. When encapsulated within 50T hydrogels HRP had enhanced activity upon the application of denaturing heat compared to the protein encapsulated within EP hydrogels or formulated in solution (Figure 4c). Though the EP hydrogel did impart significant stabilizing effect on HRP compared to the protein solution at 70 °C, this did not match the protection afforded by the 50T hydrogel. The HRP activity preservation for EP hydrogels was lost at 80 °C, while the 50T material retained some stabilizing properties. When hydrogels were loaded with HRP and processed by high vacuum lyophilization for 48 h before being rehydrated for an additional 24 h period, the 50T hydrogel had significantly more preserved HRP activity compared to both the EP hydrogel and protein solution (Figure 4d). These data

suggest additional utility of the trehalose hydrogel as a way to mitigate protein damage during manufacturing processes that are relevant to numerous biopharmaceutical applications.

The mechanism by which trehalose as an osmolyte is able to stabilize proteins in solution during exposure to lyophilization stressors or extreme heat conditions remains poorly understood.[28,41] However, three main theories have emerged from a large body of physical chemistry literature that may explain the functionality of this excipient. These theories include protein stabilization via either: 1) mechanical entrapment of the protein within a glassy structure formed by the trehalose molecules as a result of their relatively high glass transition temperature (vitrification theory); 2) direct hydrogen bonding between the protein and trehalose which preserves protein structure in the absence of sufficient water (water replacement theory); or 3) by rearranging and concentrating water toward the surface of the biomacromolecule also directed by hydrogen bonding (water entrapment/preferential exclusion theory).[27] The unique strength and spatial orientation of hydrogen bonding provided by trehalose is therefore believed to play an important role in protein stabilization. Thus, understanding how these interactions are altered when trehalose is covalently incorporated within the hydrogel is critically important to elucidating its mechanism of action in these materials. We used attenuated total reflection Fourier transform infrared (ATR-FTIR) spectroscopy to characterize the hydrogen bonding within the hydrogel (Figure 5a), with a focus on the spectral signal within the OH stretch region (3000–3800 cm^{-1}) being used to evaluate the specific nature and strength of this bonding as a result of TDA inclusion. The study of hydrogen bonding using ATR-FTIR requires dehydration of the hydrogel matrix, and while direct in situ conditions cannot be evaluated, important information pertaining to the hydrogen bonding interactions can still be garnered by maintaining minimal network hydration. To prepare semidry hydrogel materials, we dehydrated samples under modest house vacuum conditions for 24 h in the absence of a desiccant. To increase the extent of hydrogel drying we made use of calcium sulfate desiccant and/or high vacuum sources to establish greater anhydrous conditions. Interestingly, under semidry conditions trehalose hydrogels demonstrated uniquely strong and ordered hydrogen bonding which was observed as a characteristic three-principle mode distribution within the OH stretch region formed by three overlapping bands at 3290, 3450, and 3510 cm^{-1} (Figure 5a). The 3290 cm^{-1} νOH stretch indicates the existence of strong interchain hydrogen bonding interactions likely between trehalose hydroxyls (hydrogen donor) and carbonyl groups (hydrogen acceptor) that are present within the hydrogel network.[42,43] By contrast the other νOH stretches at 3450 and 3510 cm^{-1} are likely attributable to intramolecular interactions between trehalose hydroxyls along with their interaction with ether groups on the PEG chains derived from the TMPE-TL and PEGDA.[44] The pattern of hydrogen bonding was similar for all trehalose-containing hydrogels and the strength of these vibration modes was linearly dependent on TDA composition, suggesting direct involvement of the trehalose molecules in this bonding (Figures 5b and S14, Supporting Information). In samples exposed to increasingly strenuous drying conditions the multimodal νOH signal transitioned into a higher wavenumber and a more broadly distributed hydrogen bonding pattern evident as a single mode centered at 3350 cm^{-1} (Figures 2c and S15, Supporting Information). The lower wavenumber and

decreased bandwidth of the *ν*OH stretch with greater water content suggest that the coupled vibrations associated with these hydrogen-bonding interactions are stronger in the presence of some hydration with a higher degree of homogeneity within the matrix that appears to be water assisted.[44,45] Variations in the hydrogen-bonding distribution as a function of hydration for the trehalose hydrogel were also reflected in mechanical property differences (Figure S16, Supporting Information). When fully hydrated 50T hydrogels were equilibrated at 37 °C and then tested under uniaxial mechanical compression, the compressive modulus (47.42 kPa) was approximately 2.9 times more compliant than the EP hydrogel that contained no trehalose (137.6 kPa). However, upon drying to the semidry state the difference in mechanical properties between the two samples was incredible, with the 50T hydrogel demonstrating stiffness and strength that was over an order of magnitude greater than the EP hydrogel while also displaying a profile more reminiscent of a thermoplastic elastomer (TPE) than that of a classic rubber/elastomer material (Figure S16, Supporting Information). However, the TPE-like character displayed by the 50T hydrogel was lost upon further drying at which point the materials mechanical properties were approximately equivalent to the dry EP hydrogel. These mechanical testing data provide evidence that water within the trehalose hydrogels acts as either a plasticizing or an antiplasticizing agent depending on the extent of hydration, in a manner similar to that described previously for other carbohydrate–polymer–polyol glassy matrices.[45,46] These data confirm that trehalose hydrogels possess unique long-range ordered hydrogen bonding domains throughout the network that is maximized at a certain level of hydration where free water within the network is almost entirely removed and the residual water is compartmentalized within intramolecular hydrogen bonding. The compartmentalized water acts as an antiplasticizing agent enhancing the molecular packing and consequently mechanical properties of the network.

The inclusion of trehalose as an osmolyte dispersed within EP hydrogels did not display the same hydrogen-bonding pattern as seen for covalent incorporation, and instead there was a broad and much less intense spectra for the equivalent molar concentration of hydroxyl groups suggesting a heterogeneous distribution of hydrogen bonding (Figure 5d). For comparisons, hydrogels containing an alternate free polyol distribution within the network at equivalent molar concentration were prepared through the reaction of TMPE-TL, TMPE-triacrylate, and thioglycerol. This thioglycerol hydrogel containing pendant hydroxyls within the network had a broadly distributed pattern of hydrogen bonding with a single band at a higher wavenumber (3500 cm^{-1}) (Figure 5d). Disaccharide trehalose is known to have a stronger propensity for forming intermolecular hydrogen bonding as well as interacting more favorable with water molecules compared to other similar-sized sugars and polyols.[47,48] Our analysis confirms that this specific polyol identity, orientation, and distribution, which is preserved upon covalent trehalose incorporation within hydrogels, creates exceptionally strong hydrogen bonding within the network that cannot be matched by other hydroxyl-containing entities. The strength of the multimodal hydrogen bonding in the trehalose hydrogels decreased over time and transitioned into a higher wavenumber, longer bandwidth single mode signal by 8 d in vitro (Figure 5e). This modulated signal coincided with an increase in the carboxylate (1550–1610 cm^{-1}) stretch (Figure S5, Supporting Information), suggesting that network hydrolysis and the resultant carboxylate anions generated act to redistribute the hydrogen bonding seen within the network. This

could have implications for the long-term stabilization of protein therapeutics as during hydrogel degradation the loss of strong hydrogen bonding may contribute to protein destabilization and/or aggregation.

In summary, we have demonstrated that covalent incorporation of trehalose, a recognized protein excipient, into a hydrogel network resulted in enhanced long-term functional activity of a number of fragile proteins during controlled release both in vitro and in vivo. Furthermore, upon application of relevant formulation and manufacturing stressors the trehalose hydrogel provided protection of a model protein in its active state. The mechanism by which trehalose hydrogels stabilize proteins remains to be completely elucidated. However, we have identified a uniquely strong hydrogen bonding character within the trehalose hydrogel network that was hydration dependent, which could contribute to this stabilization effect in a manner that is consistent with previously described water replacement and/or entrapment theories for osmolyte trehalose. The favorable hydrogen bonding attributable to trehalose may be amplified upon covalent incorporation of the sugar into the current hydrogels as the Michael addition step growth polymerization chemistry used here is known to provide enhanced network homogeneity and cooperativity.[49] This study supports the covalent incorporation of trehalose within hydrogels for structural stabilization of encapsulated proteins during long-term controlled release. Future evaluations with various classes of therapeutic proteins would ideally establish the modularity of this approach. For situations requiring more prolonged release, the development of trehalose hydrogels with slower degradation kinetics, perhaps by using nonester-based thiol crosslinkers, may be advantageous. Overall, the strategy outlined here has great potential to improve local delivery for numerous therapeutic applications and could help to overcome hurdles to clinical translation that arise from structural stability limitations of fragile protein therapeutics.

Experimental Section

Materials

Trehalose dihydrate (#T0167), vinyl acrylate (#771422), Lipase B acrylic resin from Candida antarctica (CALB) (#L4777), trimethylopropane ethoxylate (#416177), ethyl thiolactate (#W327905), ethyl thioglycolate (#E34307), polyethylene diacrylate (PEGDA) (M_n = 575 g mol^{-1}) (#437441), activated alumina Brockman I (basic and neutral), Filter agent Celite 545, solvents (dichloromethane, methanol, ethyl acetate, acetone, dimethyl sulfoxide), 3A and 4A molecular sieves, horseradish peroxidase (#77332, 156 U mg^{-1}), glucose oxidase from *Aspergillus Niger* (#49180, 192 U mg^{-1}), α-Chymotrypsin from bovine pancreas (#C3142), 3,3′,5,5′-Tetramethylbenzidine (TMB) Liquid Substrate System for ELISA (#T0440), D-(+)-glucose anhydrous, *N*-Succinyl-Ala-Ala-Pro-Phe p-nitroanilide (#S7388, chymotrypsin substrate), 2 N HCl solution, Tris hydrochloride (Tris-HCl), calcium chloride ($CaCl_2$) were all purchased from Sigma-Aldrich (St. Louis, MO, USA). Phosphate buffered saline pH = 7.4, FITC labeled ovalbumin, IgG-Alex Fluor 647 and Amplex UltraRed reagent were purchased from Life Technologies (Grand Island, NY, USA). Disposable 40 and 80 g HP Silica Gold Cartridges were purchased from Teledyne Isco (Lincoln, NE, USA).

Instrumentation

Purity and extent of functionalization of all synthesized hydrogel precursor molecules was confirmed by liquid chromatography–mass spectrometry (LC–MS) and ^{1}H NMR. For LC–MS analysis of trehalose diacrylate, samples were loaded at a 1 mg mL^{-1} concentration and run through a UPLC BEH C18, 1.7 μL, 2.1 mm × 50 mm column at a rate of 0.6 mL min^{-1}. The mobile phase used was a 3 min gradient of HPLC grade water and acetonitrile with 0.01% formic acid. Eluted products were characterized by UV-PDA detector and ESI QT of MS.^{1}H NMR spectra of trehalose diacrylate were recorded on a Bruker 400 MHz NMR spectrometer using the residual proton resonance of the deuterium oxide as the internal standard. Chemical shifts were reported in parts per million (ppm). Dynamic Rheology was performed on mixed hydrogel solutions to monitor the sol–gel transition. Using an ARES G2 rotational rheometer (TA Instruments, New Castle, Delaware) 300 μL of hydrogel mixture was applied to a temperature-controlled stage set at 37 °C. A 25 mm parallel stainless-steel plate geometry was used for all tests and dynamic time sweep measurements were made within the linear viscoelastic region at 5% strain and a frequency of 10 rad s^{-1}. Fourier transform infrared spectroscopy (FTIR) was used to characterize the trehalose hydrogels. Using an Eco-ATR module attachment to an ALPHA FT-IR Spectrometer (Bruker) the FTIR spectra of pressed dried hydrogel discs were recorded at 2 cm^{-1} intervals with a minimum of 80 repeat measurements. The ester stretch (≈1730 cm^{-1}) was used to normalize the absorbance readings between hydrogel samples. The hydrogen bonding within the samples was analyzed using the OH stretch spectral region (3000–3800 cm^{-1}), while the carboxylate stretch was assessed at 1550–1610 cm^{-1}. Integration of spectra peaks was performed using the Bruker OPUS software. To perform compressive mechanical testing on the EP and trehalose hydrogels, a 5943 single column table top mechanical testing system (Instron) was used. Cylindrical samples (diameter = 3 mm; height = 5 mm) that had been incubated in PBS at 37 °C were used to test the strength of equilibrated hydrogels. Samples with the same dimensions were dried under the various conditions described in the Results and Discussion section of this paper to obtain semidry and dry networks. For all samples tested a crosshead compression rate of 5 mm min^{-1} was used and the resistive force was recorded using a 10 N load cell.

Synthesis of Trehalose Diacrylate

Selective acrylation of trehalose was performed using an enzymatic-catalyzed reaction similar to previously reported.[29] Briefly, trehalose diacrylate was synthesized by reacting a 4 mole excess of vinyl acrylate (48 mmols, 5 mL) with trehalose dihydrate (16 mmols, 4.1 g) in the presence of CALB (1 g) in dry acetone (500 mL) at 50 °C and 250 rpm for 48 h on an orbital shaker. Trace amounts of 4-methoxyphenol (MEHQ) were also added to prevent any radical homopolymerization of the product during the reaction. The crude product was filtered, concentrated in vacou and then purified via silica flash chromatography on a CombiFlash Rf system using a 40 g disposable prepacked silica gold cartridge and ethyl acetate and 80% methanol/water as the binary solvent mobile phases. Purified trehalose diacrylate was identified by thin layer chromatography (TLC) using cerium–ammonium–molybdate (CAM) stain and purified fractions were collected and dried in vacuo using a rotary evaporator. Trace amounts of MEHQ were included in the solution of combined purified fractions just prior to solvent removal to prevent radical homopolyerization. Dried

trehalose diacrylate was stored at 4 °C until use.^{1}H NMR (400 MHz, D2O, δ) 6.47 (dd, 2H), 6.24 (m, 2H), 6.02 (dd, 2H), 5.16 (d, 2H), 4.51 (dd, 2H), 4.40 (dd, 2H), 4.09 (m, 1H), 3.87 (t, 2H), 3.67 (dd, 2H), 3.54 (dd, 2H).

Synthesis of TMPE-TL and TMPE-TG

The synthesis of TMPE-TL and TMPE-TG was performed using a enzymatic-catalyzed transesterfication reaction which was described in detail by our group elsewhere.[12] Briefly, 10 g of 4A molecular sieve dried trimethylopropane ethoxylated (TMPE) was combined with a five molar excess of either ethyl 2-mercaptoproprionate (TL) or ethyl thioglycolate (TG) in a 100 mL round-bottom flask, followed by CALB (1 g). The flask was placed on a magnetic stirrer at 50 °C and allowed to react overnight under moderate vacuum conditions. The reaction was purified by silica flash chromatography on a CombiFlash Rf system using a disposable prepacked silica column (80 g) with a dichloromethane/methanol (0–10%) gradient elution method. Purified fractions were detected by UV–vis and then combined and dried in vacuo using a rotary evaporator yielding a clear viscous liquid at room temperature. Vials of TMPE-TL and TMPE-TG were stored at 4 °C under nitrogen gas and were individually flashed neat over a bed of neutral alumina prior to use. The characterization of TMPE-TL and TG by LC–MS and^{1}H NMR was described in detail by us previously.[12]

Hydrogel Fabrication

Trehalose hydrogels were prepared by combining TMPE-TL, TDA, and PEGDA 575 in PBS at a stoichiometric equivalency of thiol groups to acrylate groups in a manner similar to previous studies.[12] Briefly, PEGDA, a liquid at room temperature, was first flashed neat over activated basic alumina to remove the MEHQ inhibitor added by the manufacturer. Weighed masses of TDA and PEGDA were solubilized with an appropriate volume of PBS and placed on ice for 10 min. The volume of PBS added to the TDA/PEGDA solution was sufficient to obtain a 25 wt% hydrogel. The relative amounts of TDA and PEGDA used to make the hydrogels depended upon the specific trehalose content of the hydrogel. Hydrogels were fabricated by adding the TDA/PEGDA solution to a weighed quantity of TMPE-TL. To make EP hydrogels a similar procedure was used except that a solution of PEGDA only was added to a blended quantity of TMPE-TG and TMPE-TL.

In Vitro Protein Release Studies

Model protein controlled release was investigated by encapsulating FITC-labeled Ovalbumin (45 kDa), and Alexa Fluor 647 IgG (150 kDa) into hydrogels at 1 mg mL^{-1}. Hydrogels were incubated in 1 mL of PBS and replaced daily. Protein concentration was read on an Infinite M1000 PRO microplate reader (Tecan) using appropriate fluorophore excitation and emission wavelengths (ex/em 490/525 for FITC; ex/em 650/668 for Alea Fluor 647). An eight-sample serially diluted standard curve was generated for each protein in order to convert the microplate read fluorescent intensity into a protein concentration value.

Protein Activity Assays

Horseradish peroxidase (HRP), glucose oxidase (GOx), and α-chymotrypsin were all used as received from the vendor without any further purification. For the active protein recovery

assays proteins were loaded into 60 μL hydrogel discs (≈5 mm diameter × 3 mm height) at concentrations ranging from 500 μg mL^{-1} to 2 mg mL^{-1} and incubated in 600 μL of PBS/0.01% BSA in a 48-well microplate that was shaken at 37 °C and 150 rpm on an orbital shaker. Hydrogel samples were run in groups of three or four for all assays. The incubation media was replaced daily and the recovered incubation media was analyzed for protein activity. For the HRP activity assay, samples were first diluted in Hanks balanced salt buffer (HBSS) (1/50 dilution) to obtain a concentration that was within the linear range of the TMB colorimetric assay. To perform the TMB colorimetric assay 50 μL of diluted recovered incubation media was added to 50 μL of TMB substrate within a 96-well microplate and was developed at 37 °C for 5 min before adding 100 μL of 2 N HCl to stop the enzymatic reaction. The colorimetric intensity of samples was read on a microplate reader at 450 nm with absorbance at 540 nm used as a reference. For each daily measurement an eight-sample serially diluted standard series was used for HRP concentration calculations. For the GOx activity assay recovered aliquots were diluted at 1/20 in PBS and 50 μL of the diluted solution was added to an individual well of a 96-well plate. The Amplex Red substrate solution was prepared by combining 50 μL of 10×10^{-3} M Amplex Red Stock in DMSO, 100 μL of 100 μg mL^{-1} HRP, 1.25 mL of 400×10^{-3} M glucose stock and 3.6 mL of PBS. 50 μL of the Amplex Red substrate was added to the diluted aliquots to initiate the enzymatic reaction and the developing pink color was monitored at discrete time intervals on a microplate reader at wavelength of 560 nm. A 12-sample serially diluted standard series from 2.5 μg mL^{-1} was used to calculate active GOx concentrations. For the α-chymotrypsin assay, hydrogel incubation media was recovered and diluted as needed. The substrate solution was prepared by solubilizing the *N*-Succinyl-Ala-Ala-Pro-Phe p-nitroanilide substrate at a 2×10^{-3} M concentration in 0.2 M Tri-HCl/20×10^{-3} M $CaCl_2$ pH = 7.8 buffer. A 100 μL aliquot of the substrate was added to 100 μL of the sample aliquot and the developing yellow hue was read at 410 nm on a microplate reader continuously over a 10 min period. An eight-sample serially diluted standard curve was generated to calculate active recovered protein. For measurements of active HRP within hydrogels, 15 μL hydrogel discs were removed from either in vitro or in vivo conditions at defined time points, washed once in HBSS, and then incubated in 50 μL of fresh HBSS before application of 50 μL TMB substrate. At defined time points the enzymatic reaction was stopped by applying 100 μL of 2 N HCl and hydrogels were removed from the microplate before the colorimetric intensity was read on a microplate reader at 450 nm with absorbance at 540 nm used as reference.

In Vivo Implantation of Hydrogels

Sterile discs (≈15 μL, 3 mm diameter, 2 mm height) of 50T and 75/25 EP hydrogels containing 2 mg mL^{-1} HRP were prepared in an autoclaved silicone mold under aseptic conditions for subcutaneous implantation in 8 week old male C57BL/6J mice. To implant hydrogels, animals were anesthetized by isoflurane inhalation and a small dorsal incision was made. A pocket in the subcutaneous space was created by blunt dissection. Six animals received five single group hydrogels (three animals per hydrogel group) loaded into this space, while three other animals received six mixed hydrogels. The surgical incision was closed with sutures and the animals were provided with postsurgical analgesia. At designated time points animals were euthanized by carbon dioxide asphyxia and hydrogels were retrieved and transferred to a solution of HBSS prior to performing the HRP activity

assay. To determine the identity of hydrogels retrieved from animals receiving the mixed implants, ATR-FTIR analysis on the hydrogels post HRP activity assay was performed.

Supplementary Material

Refer to Web version on PubMed Central for supplementary material.

Acknowledgments

This work was supported in part by a gift from In Vivo Therapeutics Corporation. T.M.O would like to acknowledge the Sir John Monash Foundation for fellowship support. M.J.W. acknowledges support from the National Institutes of Health (NIDDK) through a Ruth L. Kirschstein National Research Service Award (F32DK101335).

References

1. Kaspar AA, Reichert JM. Drug Discovery Today. 2013; 18:807. [PubMed: 23726889]
2. Scott AM, Wolchok JD, Old LJ. Nat. Rev. Cancer. 2012; 12:278. [PubMed: 22437872]
3. Kariolis MS, Kapur S, Cochran JR. Curr. Opin. Biotechnol. 2013; 24:1072. [PubMed: 23587963]
4. Carter PJ. Exp. Cell Res. 2011; 317:1261. [PubMed: 21371474]
5. Leader B, Baca QJ, Golan DE. Nat. Rev. Drug Discovery. 2008; 7:21. [PubMed: 18097458]
6. Frokjaer S, Otzen DE. Nat. Rev. Drug Discovery. 2005; 4:298. [PubMed: 15803194]
7. Reichert JM. Nat. Rev. Drug Discovery. 2003; 2:695. [PubMed: 12951576]
8. Lin C-C, Anseth K. Pharm. Res. 2009; 26:631. [PubMed: 19089601]
9. Vermonden T, Censi R, Hennink WE. Chem. Rev. 2012; 112:2853. [PubMed: 22360637]
10. Langer R. Science. 1990; 249:1527. [PubMed: 2218494]
11. Censi R, Di Martino P, Vermonden T, Hennink WE. J. Controlled Release. 2012; 161:680.
12. O'Shea TM, Aimetti AA, Kim E, Yesilyurt V, Langer R. Adv. Mater. 2015; 27:65. [PubMed: 25381960]
13. Ramakrishna S, Kim Y-H, Kim H. PLoS One. 2013; 8:e54282. [PubMed: 23365657]
14. Tester NJ, Plaas AH, Howland DR. J. Neurosci. Res. 2007; 85:1110. [PubMed: 17265470]
15. Jiskoot W, Randolph TW, Volkin DB, Middaugh CR, Schöneich C, Winter G, Friess W, Crommelin DJA, Carpenter JF. J. Pharm. Sci. 2012; 101:946. [PubMed: 22170395]
16. Lin C-C, Sawicki SM, Metters AT. Biomacromolecules. 2007; 9:75. [PubMed: 18088094]
17. McCall JD, Anseth KS. Biomacromolecules. 2012; 13:2410. [PubMed: 22741550]
18. van de Wetering P, Metters AT, Schoenmakers RG, Hubbell JA. J. Controlled Release. 2005; 102:619.
19. Hammer N, Brandl FP, Kirchhof S, Messmann V, Goepferich AM. Macromol. Biosci. 2015; 15:405. [PubMed: 25399803]
20. Chen S-C, Wu Y-C, Mi F-L, Lin Y-H, Yu L-C, Sung H-W. J. Controlled Release. 2004; 96:285.
21. Koutsopoulos S, Unsworth LD, Nagai Y, Zhang S. Proc. Natl. Acad. Sci. U.S.A. 2009; 106:4623. [PubMed: 19273853]
22. Pérez C, Castellanos IJ, Costantino HR, Al-Azzam W, Griebenow K. J. Pharm. Pharmacol. 2002; 54:301. [PubMed: 11902796]
23. Lee H, McKeon RJ, Bellamkonda RV. Proc. Natl. Acad. Sci. U.S.A. 2009; 107:3340. [PubMed: 19884507]
24. Stanwick JC, Baumann MD, Shoichet MS. J. Controlled Release. 2012; 160:666.
25. Iyer PV, Ananthanarayan L. Process Biochem. 2008; 43:1019.
26. Fu K, Klibanov AM, Langer R. Nat. Biotechnol. 2000; 18:24. [PubMed: 10625383]
27. Jain NK, Roy I. Curr. Protoc. Protein Sci. 2010; 59:4.9.1.
28. Kaushik JK, Bhat R. J. Biol. Chem. 2003; 278:26458. [PubMed: 12702728]

29. John G, Zhu G, Li J, Dordick JS. Angew. Chem. Int. Ed. 2006; 45:4772.
30. Taguchi H, Sunayama H, Takano E, Kitayama Y, Takeuchi T. Analyst. 2015; 140:1448. [PubMed: 25629605]
31. Mao L, Luo S, Huang Q, Lu J. Sci. Rep. 2013; 3:3126. [PubMed: 24185130]
32. Veitch NC. Phytochemistry. 2004; 65:249. [PubMed: 14751298]
33. Szigeti K, Smeller L, Osváth S, Majer Z, Fidy J. Biochim. Biophys. Acta. 2008; 1784:1965. [PubMed: 18805513]
34. Hassani L, Ranjbar B, Khajeh K, Naderi-Manesh H, Naderi-Manesh M, Sadeghi M. Enzyme Microb. Technol. 2006; 38:118.
35. Mancini RJ, Lee J, Maynard HD. J. Am. Chem. Soc. 2012; 134:8474. [PubMed: 22519420]
36. Lee J, Lin E-W, Lau UY, Hedrick JL, Bat E, Maynard HD. Biomacromolecules. 2013; 14:2561. [PubMed: 23777473]
37. Bat E, Lee J, Lau UY, Maynard HD. Nat. Commun. 2015; 6:6654. [PubMed: 25791943]
38. Chattopadhyay K, Mazumdar S. Biochemistry. 2000; 39:263. [PubMed: 10625502]
39. Fu L, Liu J, Yan ECY. J. Am. Chem. Soc. 2011; 133:8094. [PubMed: 21534603]
40. Schuler B, Hofmann H. Curr. Opin. Struct. Biol. 2013; 23:36. [PubMed: 23312353]
41. Singer MA, Lindquist S. Mol. Cell. 1998; 1:639. [PubMed: 9660948]
42. Imamura K, Ohyama K-i, Yokoyama T, Maruyama Y, Imanaka H, Nakanishi K. J. Pharm. Sci. 2008; 97:519. [PubMed: 17724665]
43. Taylor LS, Zografi G. J. Pharm. Sci. 1998; 87:1615. [PubMed: 10189276]
44. Wolkers WF, Oliver AE, Tablin F, Crowe JH. Carbohydr. Res. 2004; 339:1077. [PubMed: 15063194]
45. Roussenova M, Murith M, Alam A, Ubbink J. Biomacromolecules. 2010; 11:3237. [PubMed: 21049921]
46. Roussenova M, Andrieux J-C, Alam MA, Ubbink J. Carbohydr. Polym. 2014; 102:566. [PubMed: 24507320]
47. Wyatt TT, van Leeuwen MR, Golovina EA, Hoekstra FA, Kuenstner EJ, Palumbo EA, Snyder NL, Visagie C, Verkennis A, Hallsworth JE, Wösten HAB, Dijksterhuis J. Environ. Microbiol. 2015; 17:395. [PubMed: 25040129]
48. Jain NK, Roy I. Protein Sci. 2009; 18:24. [PubMed: 19177348]
49. Tibbitt MW, Kloxin AM, Sawicki LA, Anseth KS. Macromolecules. 2013; 46:2785.

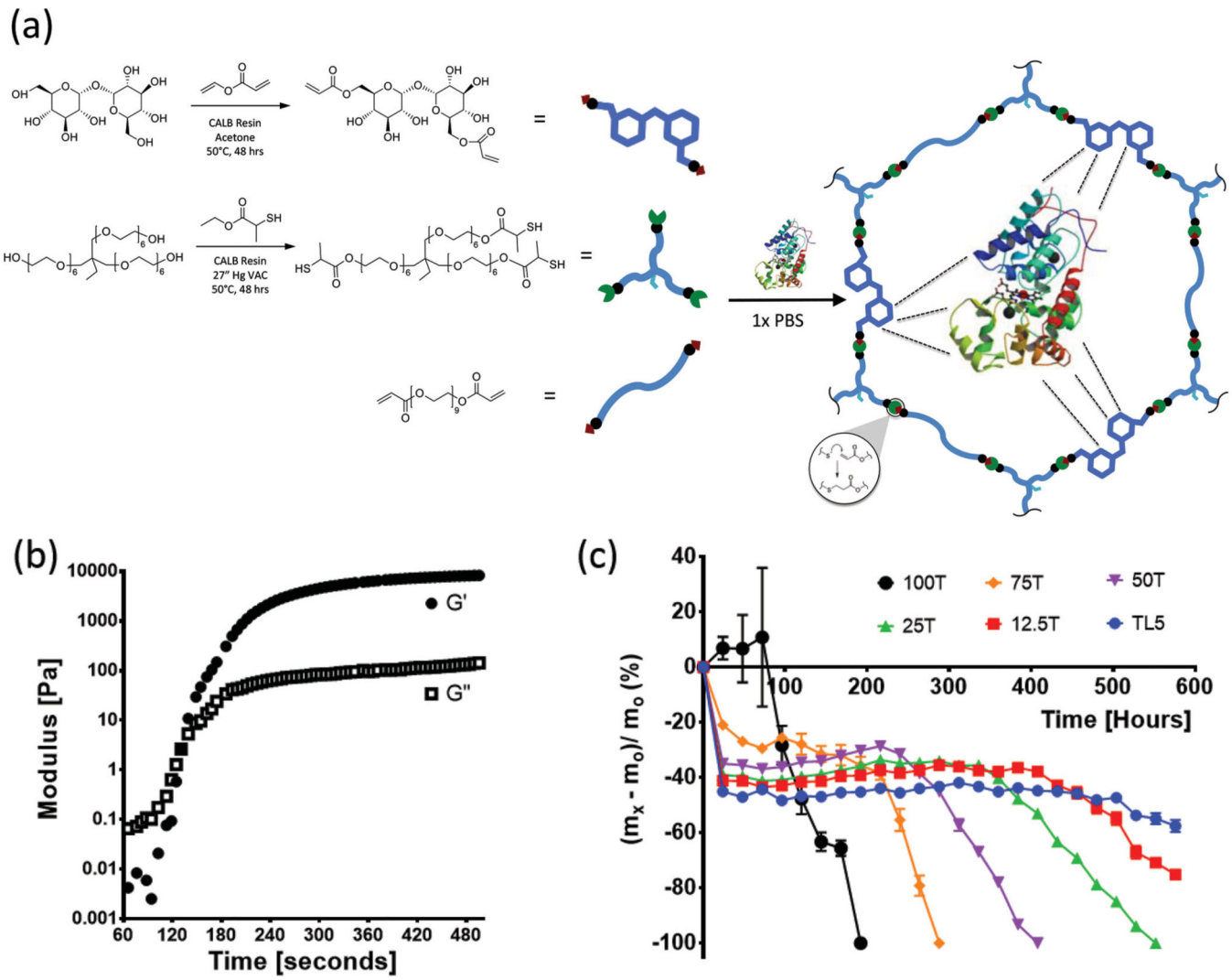

Figure 1.

Trehalose hydrogels formulated using thiol-acrylate Michael addition chemistry. a) Overview of trehalose diacrylate (TDA) and TMPE-TL synthesis both using CALB resin as a catalyst. Combining TMPE-TL, TDA, and PEGDA in PBS allows a hydrogel to form that can encapsulate and stabilize protein therapeutics. b) Dynamic rheology curve for 100T hydrogel (strain = 5%, frequency = 10 rad s^{-1}). c) Percentage hydrogel wet mass changes (compared with the initial cured wet mass) over time for hydrogels with various percentage compositions of trehalose within the network (TL5 = TMPE-TL PEGDA 575).

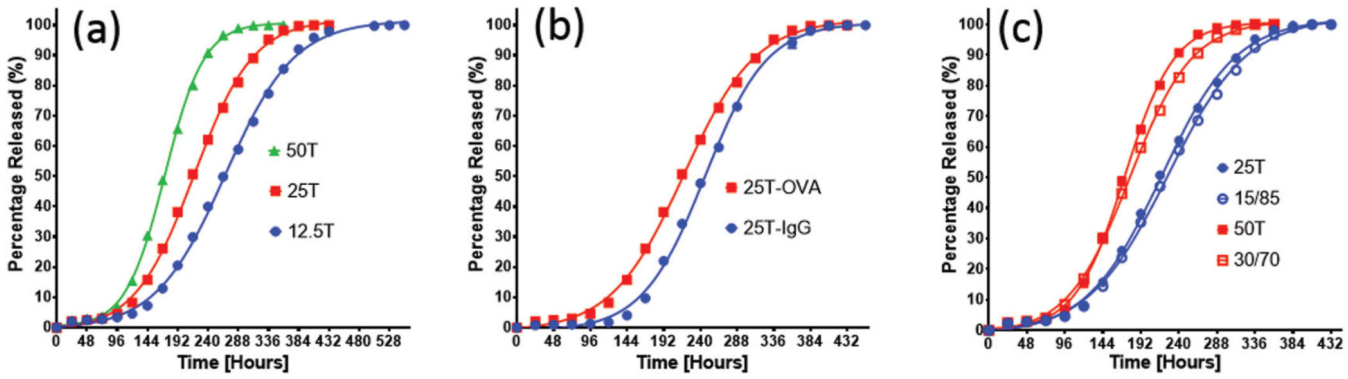

Figure 2.

Controlled release of model proteins from trehalose hydrogels. a) Cumulative FITC-ovalbumin release profiles from various percentage compositions of trehalose within hydrogels; b) comparative cumulative release profile for 25T hydrogels encapsulating FITC-ovalbumin and Alexa Fluor 647 IgG; c) blended TMPE-TG/TL 575 EP hydrogel formulations show equivalent release profiles for certain trehalose hydrogels.

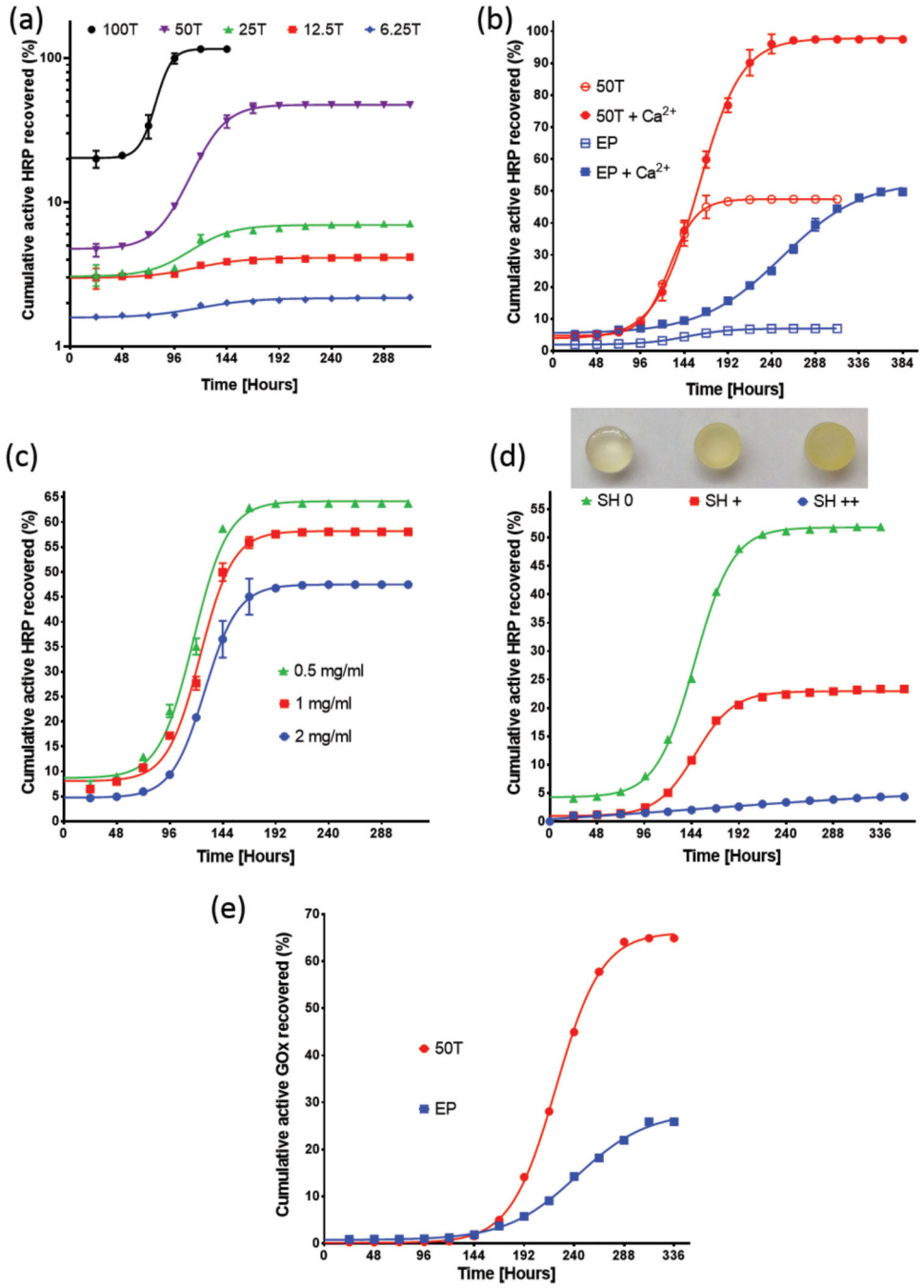

Figure 3.

Trehalose hydrogels show greater recovery of active proteins during controlled release. a) Cumulative HRP recovery for hydrogels with various percentage compositions of trehalose. (note: the *y*-axis is represented on a log scale for ease of visualization of the different release curves). b) Comparison of cumulative HRP recovery for 50T and EP hydrogels released into PBS and media containing 1×10^{-3} M $CaCl_2$. c) Cumulative HRP recovery for various HRP loading concentrations within 50T hydrogels. d) Effect of excess free thiol groups within 50T hydrogels on cumulative HRP recovery. The image above the graph shows hydrogels

stained with Ellman's reagent, with increased yellow hue within the materials demonstrating higher free thiol content. e) Comparison of cumulative GO recovery for 50T and EP hydrogels loaded releasing into PBS.

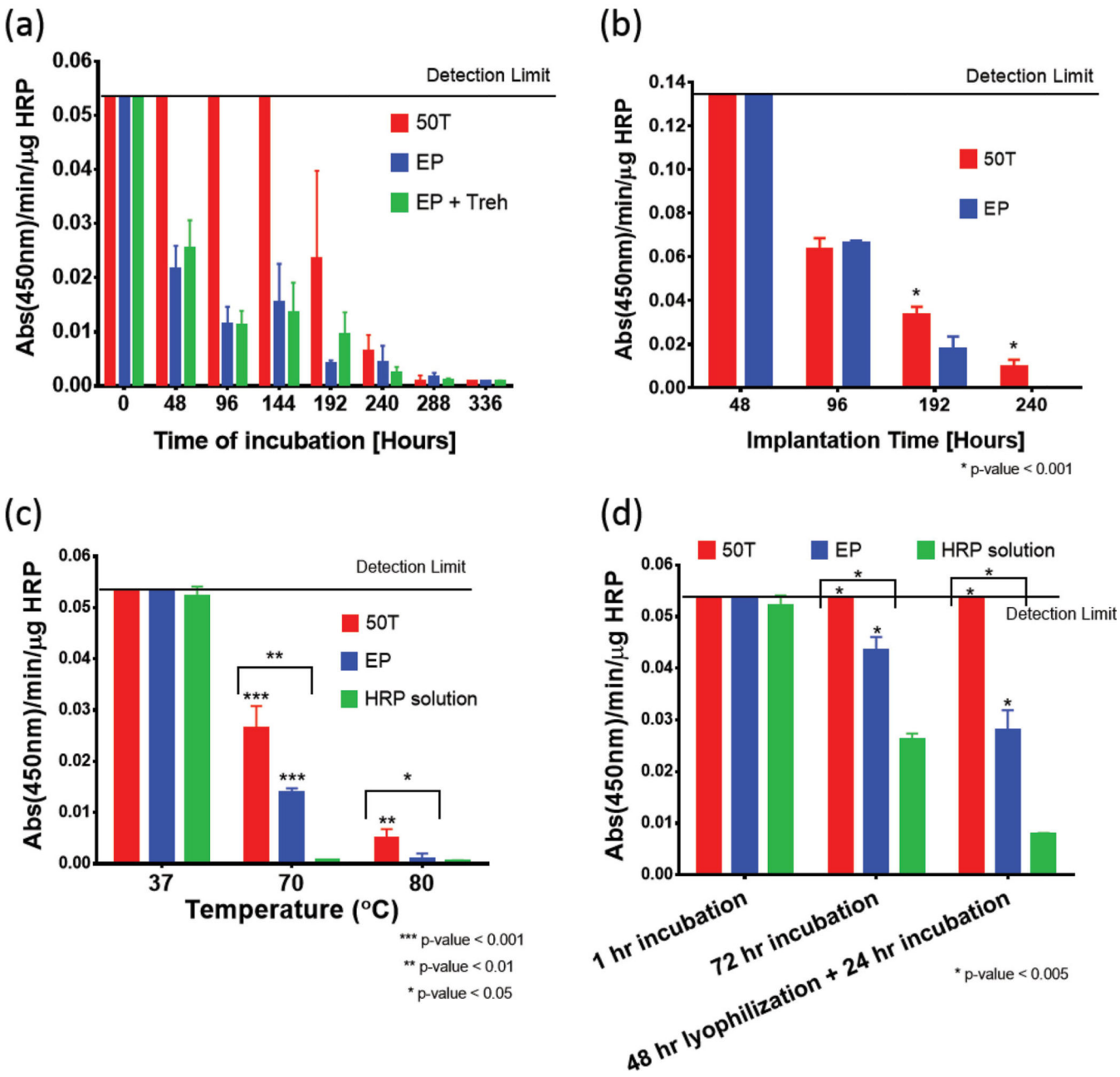

Figure 4.

Measuring HRP stability within trehalose hydrogels. a) Comparison of HRP activity within hydrogels incubated in PBS in vitro. b) Comparison of HRP activity within hydrogels implanted in vivo within the subcutaneous space of mice. Effect of trehalose hydrogels on preventing loss of encapsulated HRP activity upon c) 1 h incubation in denaturing temperatures; and d) 48 h lyophilization and subsequent rehydration for 24 h.

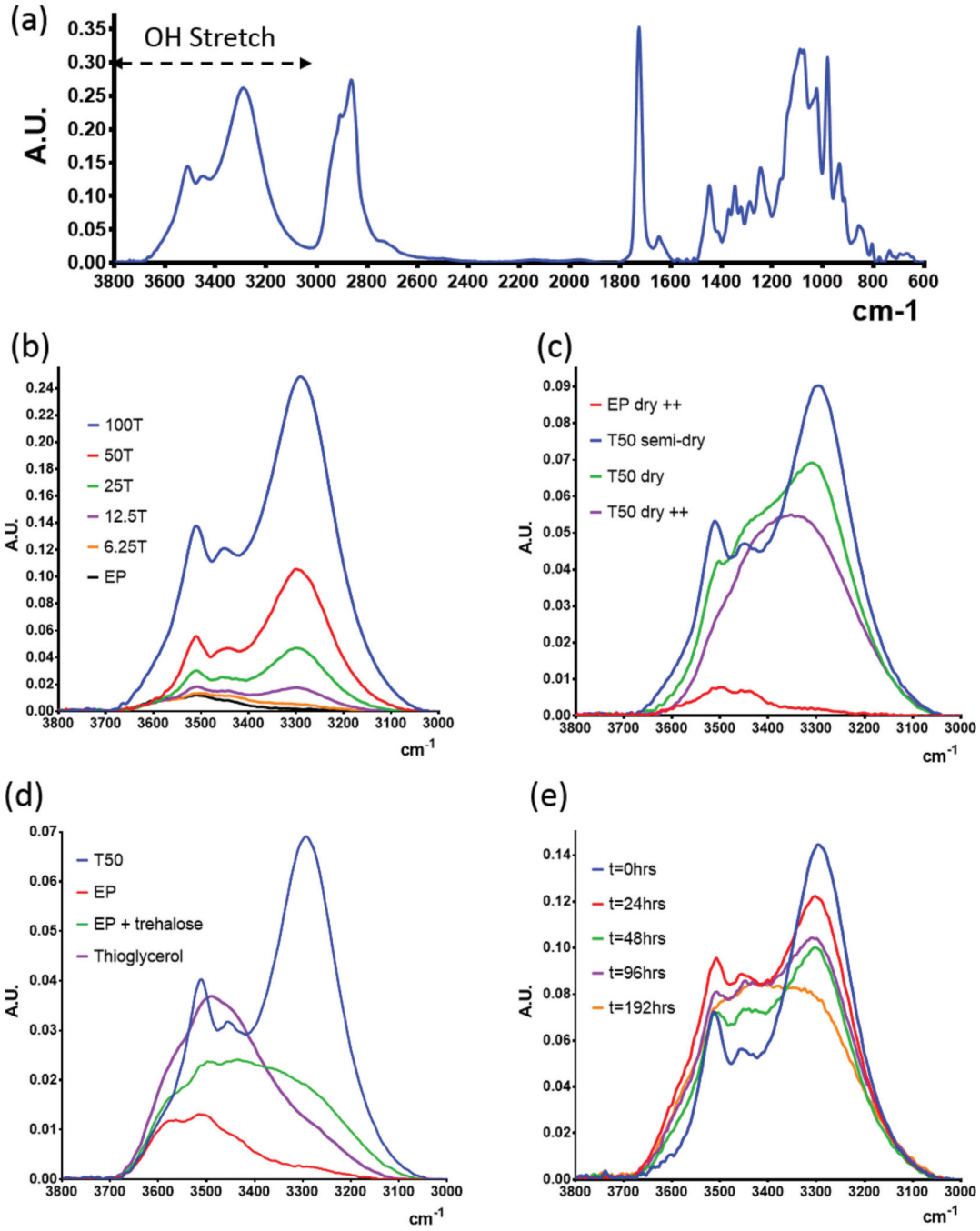

Figure 5.

Trehalose hydrogels display unique, strong hydrogen bonding. a) Complete ATR-FTIR of a semidry 100T hydrogel. ATR-FTIR OH stretch spectra for: b) semidry hydrogels with various percentage compositions of trehalose (all spectra normalized at the ester peak ≈1730 cm^{-1}); c) 50T hydrogels with varied levels of hydration; d) comparison of semidry hydrogels containing different polyol distributions within the hydrogel network; and e) semidry 50T hydrogels incubated in PBS for different periods of time.